Research Article

Received: 24 September 2023 Revised: 13 May 2024 Published online in Wiley Online Library:

(wileyonlinelibrary.com) DOI 10.1002/jctb.7695

N-Acetyl cysteine-loaded liposomes to reduce iron overload-induced toxicity in human kidney cells

Doohee Lee,[a] Chaewon Bae,[b] Suhyun Ryu[a] and Kangwon Lee[a,c*]

Abstract

BACKGROUND: Iron overload in the body generates free radicals through the Fenton reaction, leading to adverse effects on various organs. Several antioxidants have been recommended to treat iron-related diseases effectively. *N*-Acetyl cysteine (NAC), a potent antioxidant, was investigated in this study for its potential to mitigate iron overload-induced cell death. A liposomal formulation was developed to encapsulate NAC, employing the reverse phase evaporation method, to enhance its delivery and effectiveness. The liposomal NAC was characterized by evaluating its size, zeta potential, morphology and release profiles.

RESULTS: The protective effect of liposomal NAC against iron overload-induced toxicity was assessed in human kidney 2 (HK-2) cells. Cell viability assays (Cell Counting Kit 8) and reactive oxygen species assays (DCFDA assay) confirmed the effectiveness of liposomal NAC in inhibiting ferroptosis induced by slow iron uptake (1 mmol L^{-1} ferric ammonium citrate). Additionally, liposomal NAC protected cells from toxicity resulting from rapid iron uptake (50 μmol L^{-1} ferric ammonium citrate, 20 μmol L^{-1} 8-hydroxyquinoline). The liposomal formulation demonstrated an enhanced protective effect compared to free NAC.

CONCLUSION: These findings suggest that liposomal NAC more effectively protects human kidney cells from toxicity caused by different iron uptake models than free NAC, highlighting its potential as a superior treatment option for iron overload-induced cellular damage.

Supporting information may be found in the online version of this article.

Keywords: liposome; iron; *N*-acetyl cysteine; ferroptosis; kidney; reactive oxygen species

INTRODUCTION

Iron is one of the fundamental elements that need to be maintained for homeostasis in the human body. Iron overload is known to have some adverse effects on the heart, pancreas, kidney, etc.[1] Non-transferrin-bound iron (NTBI) refers to iron in the bloodstream that is not bound to transferrin, the main iron transport protein. Elevated levels of NTBI increase the intracellular labile iron pool (LIP), and the enhanced LIP induces reactive oxygen species (ROS) by the Fenton reaction. ROS, as highly reactive molecules, induce cellular damage through oxidative modifications of proteins, leading to functional impairment or degradation. Moreover, ROS inflict detrimental effects on DNA integrity and cell membranes, perturbing critical cellular processes and culminating in apoptotic or necrotic cell death pathways.[1-3] Some reports mentioned that ferroptosis seems to be a leading cell death mechanism in iron overload-induced cell death.[4,5]

Ferroptosis is a recently discovered form of programmed cell death characterized by iron-dependent lipid peroxidation, occurring through the Fenton reaction of iron metabolism. This process is distinct from other forms of cell death due to its unique reliance on iron and its associated oxidative stress, making it particularly relevant in conditions of iron overload.[6] Typically, patients use iron chelators to lower excessive plasma iron levels and prevent the toxicity of iron overload. Excessive iron levels in humans are generally considered to be serum ferritin concentrations above 300 μg L^{-1} for men and 200 μg L^{-1} for women, or transferrin saturation greater than 45%. However, iron chelators are reported to have side effects such as acute renal failure, liver failure, hearing loss, and visual loss.[3,7,8] So, various antioxidants such as curcumin and histidine have been studied as alternative treatments.[9,10]

* *Correspondence to: K Lee, Department of Applied Bioengineering, Graduate School of Convergence Science and Technology, Seoul National University, Seoul 08826, Republic of Korea, E-mail: kangwonlee@snu.ac.kr*

a *Department of Applied Bioengineering, Graduate School of Convergence Science and Technology, Seoul National University, Seoul, Republic of Korea*

b *Program in Nanoscience and Technology, Graduate School of Convergence Science and Technology, Seoul National University, Seoul, Republic of Korea*

c *Research Institute for Convergence Science, Seoul National University, Suwon-si, Republic of Korea*

In the context of iron overload, *N*-acetyl cysteine (NAC) emerges as a potential candidate for protecting cells from iron overload-induced cell death. *In vitro* studies often use iron concentrations ranging from 100 to 200 μmol L^{-1} to simulate conditions of iron overload, mimicking the elevated levels found in pathological states. NAC is a well-known medication to treat paracetamol poisoning or mucolytic therapy.[11] It is selected as one of the World Health Organization's Lists of Essential Medicines.[12] Furthermore, it is low-priced and easily accessible, and has relatively few side effects.[11,12] Moreover, NAC functions as a prominent antioxidant drug in both indirect and direct manners. Indirectly, NAC is converted to L-cysteine inside cells, and L-cysteine is a rate-limiting factor to the synthesis of glutathione (GSH). So, a supply of NAC to cells can help replenish GSH, and synthesized GSH increases the antioxidant activity of the GPX4 enzyme.[13-15] This mechanism of NAC can inhibit lipid peroxidation and eventually prevent ferroptosis.[6] NAC also can scavenge free radicals directly because its thiol group can work as a source of reducing agents.[16] However, NAC has a short half-life and low bioavailability, so its use requires repeated and higher dosing.[17] Numerous studies have shown that NAC delivery by liposomal form makes the drug slowly released, prolongs blood circulation time and improves bioavailability.[18-20] In addition, liposomes possess a structure similar to that of cell membranes, which facilitates the cellular uptake of hydrophilic molecules by mimicking the cell membrane.[21] Moreover, liposomes have gained significant recognition as a safe and efficient drug delivery system. They have received approval from the US Food and Drug Administration due to their proven safety profile.[21,22] This approval has firmly established liposomes as a trusted and widely employed platform for delivering drugs.

Therefore, in the research reported here, we investigated the correlation between iron loading and ferroptosis mechanism in human kidney 2 (HK-2) cells. HK-2 cells were used because iron overload is known to induce acute renal failure as it produces oxidative stress to kidney cells.[1,3,23] And we developed liposomes that encapsulate NAC using the reverse phase evaporation (REV) method. The REV method can increase the encapsulation efficiency of hydrophilic drugs by making a water-in-oil (W/O) emulsion.[21,22,24] To confirm the feasibility in pharmaceuticals, we checked out the size, zeta potential, morphology and release profiles of the liposomes. Finally, we investigated whether liposomal NAC reduces iron overload-induced toxicity more effectively than free NAC using cell viability assay and ROS assay. Figure 1 shows an overall schematic of how liposomal NAC protects cells from toxicity caused by cellular uptake of iron.

MATERIALS AND METHODS

Materials

HK-2 cells were purchased from Korea Cell Line Bank (Gyeonggi-do, Korea). NAC, sodium bicarbonate, cholesterol, ammonium iron(III) citrate (FAC), 1,2-dipalmitoyl-*sn*-glycero-3-phosphocholine (DPPC), 8-hydroxyquinoline (8-Hq), liproxstatin-1, ferrostatin-1, necrostatin-1 and Z-VAD-FMK were all obtained from Sigma-Aldrich Company (St Louis, USA). Chloroform (99.8%) and dimethylsulfoxide (99.8%) were obtained from Samchun (Gyeonggi-do, Korea).

Preparation of liposomal NAC

Liposomes were fabricated with reference to a previously reported REV method[24] but with modifications. An organic solvent was prepared by dissolving 7 mmol L^{-1} of DPPC and 3 mmol L^{-1} of cholesterol in chloroform. An aqueous solution was then prepared by dissolving 0.067 g mL^{-1} of NAC in 1× DPBS with 0.7 mol L^{-1} sodium bicarbonate. And the two solvents were separately added in glass vials to make an aqueous-to-organic phase ratio of 1:3. The solution was sonicated using a 6 mm probe tip sonicator (VC-750, Sonics and Materials, Newtown, USA) for 5 min with pulse on for 5 s and pulse off for 10 s at an amplitude of 40% to make a W/O emulsion. After sonication, a cloudy homogeneous solution was formed, and the homogeneous state was confirmed to be maintained for more than 30 min. Then, nitrogen gas was slowly purged into the solution to evaporate chloroform overnight. The remaining viscous gel was formed. The aqueous solution was added to rehydrate it and then vigorously mixed using a homogenizer (HS-30E, DAIHAN, Daejeon, Korea) until a transparent liposome solution was seen. The liposome solution was sequentially extruded through a polycarbonate filter (Avanti Polar Lipids, Alabama, USA) of 400 and 200 nm in diameter using a mini-extruder (Avanti Polar Lipids, Alabama, USA) at above the phase transition temperature of DPPC (41 °C). The centrifugal ultrafiltration method was performed with an Amicon Ultra-15 centrifugal filter unit (MWCO 50 kDa, Merk Millipore, MA, USA) to purify the liposomes from the unentrapped drug. The liposomes were loaded into the centrifugal filter device and centrifuged at 5000 × *g* for 30 min. Control liposomes were fabricated using the above method without drugs. Finally, the made liposomes were stored at 4 °C in darkness.

Measurement of size intensity and zeta potential of liposomes

A Zetasizer Nano (Malvern, UK) was used to determine the size distribution and zeta potential of liposomes. Samples were maintained with a fixed scattering angle of 173° at 25 °C, and deionized water was used to disperse the samples.

Morphology of liposomal NAC

The morphology of liposomes was analyzed using high-resolution transmission electron microscopy (TEM; JEM-3010, JEOL Ltd, Japan). An amount of 5 μL of liposomes was dropped on a copper grid, and negative staining was done by 5 μL of 2% (w/v) sodium phosphotungstate solution.

Release profile of drugs

After purification of liposomes using the ultrafiltration method, the purified liposomes were put into a dialysis bag (1000 Da MWCO). The dialysis bag was immersed in 5 mL of DPBS at 37 °C in darkness and gently shaken at 80 rpm. At each time point, 10 μL of the sample was taken, and the amount of released drug was determined. The amount of drug was measured in triplicate at 200 nm using a NanoDrop 2000 spectrophotometer (Thermo Fisher Scientific, USA).

Cell culture

RPMI 1640 medium (Welgene, Gyeongsan), which has 1% penicillin/streptomycin and 10% fetal bovine serum (FBS), was made to culture HK-2 cell lines. The medium was renewed every 2 to 3 days, and the incubator was maintained with an atmosphere of 5% CO_2 at 37 °C.

Measurement of cell viability

A Cell Counting Kit 8 (Dojindo Inc, Tokyo, Japan) was used to investigate cell viability. Cells were seeded at 1.5×10^4 per well in a 96-well plate. And they were maintained in RPMI medium

Journal of Chemical Technology and Biotechnology published by John Wiley & Sons Ltd on behalf of Society of Chemical Industry (SCI).

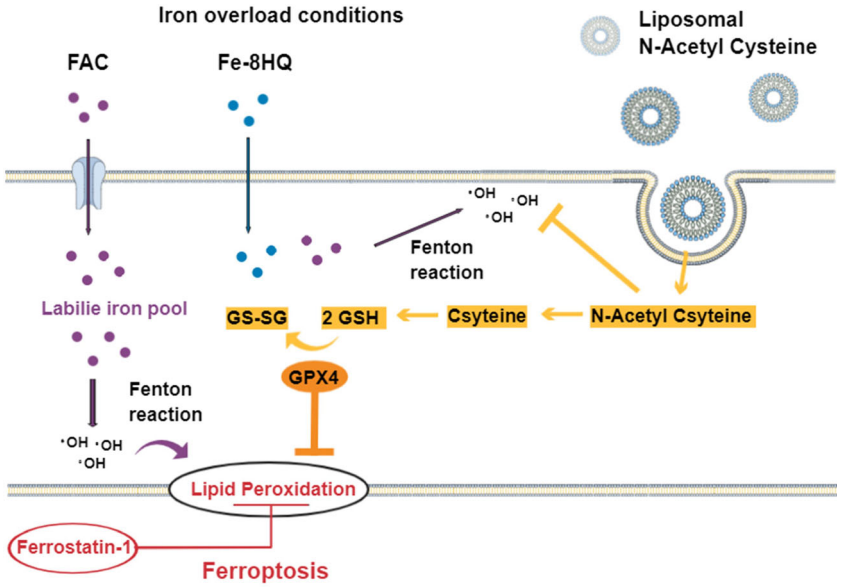

Figure 1. Schematic illustration that shows the protective effect of liposomal NAC on cell death induced by a slow or rapid increase of LIP.

without FBS. After leaving overnight, compounds were added to cells, and cells were incubated for a specific time. After the treatment, the medium was replaced with 110 µL of RPMI medium, which had 10 µL of CCK-8 solution. The experiment was done in the dark. Cells were incubated in an incubator for 3 h, and cell viability was determined from measurement of absorbance at 460 nm by a microplate reader (Synergy H1, BioTek, USA).

Quantification of reactive oxygen species

The amount of ROS released in cells was measured with a DCFDA/H2DCFDA Cellular ROS assay kit (ab113851, Abcam, Cambridge, UK). At first, 1.5×10^4 cells were seeded per well in a black 96-well microplate. After the attachment of cells, the drug of interest was treated. After a specific period, the medium was removed and washed with DPBS. The cells were stained with 25 µmol L^{-1} DCFDA solution for 45 min in an incubator. After staining, the DCFDA solution was removed and washed once, and 200 µL of DPBS was added. The fluorescence intensity was measured using a fluorescence plate reader at Ex/Em = 485/535 nm.

Statistical analysis

GraphPad Prism 8 (San Diego, USA) was used, and data are presented as mean ± SEM. A one-way analysis of variance (ANOVA) test was used to determine significant differences.

RESULTS AND DISCUSSION

Characterization of liposomal NAC

The liposomes were fabricated using the REV method making a W/O emulsion to entrap more hydrophilic drug. At first, an organic phase (phospholipids and cholesterol) and an aqueous phase (drug) were separated (Fig. 2(A)). And then, the W/O emulsion was made by sonication (Fig. 2(B)). The homogeneous state was maintained for more than 30 min, showing that the formation of the W/O emulsion is stable enough.[24] After evaporation of the organic solvent, a stable gel was formed because the liposomes are in a solid gel phase at a temperature lower than the phase transition temperature of DPPC (41 °C) (Fig. 2(C)). Finally, the liposomes were fabricated after rehydration and serial extrusions (Fig. 2(D)).

After the formation of liposomes, the morphology was confirmed by TEM (Fig. 3(A)). The morphology was spherical enough, the size being smaller than 200 nm because of the serial extrusions. An ultrafiltration process was used to purify the liposomes, and the release profile of the purified liposomes in DPBS (pH 7.4) at 37 °C was analyzed (Fig. 3(B)). After releasing the drug rapidly for 2 h, a sustained release was shown, and about 40% of the drug was released for 24 h. And then, the size and zeta potential of liposomal NAC were measured by dynamic light scattering (DLS). The Z-average size was confirmed to be 157.7 nm, and PDI is 0.217, which is small and homogeneous enough (Fig. 3(C)). The presented data showed a size smaller than 200 nm, which was similar to the size determined by TEM. This range of liposome size is appropriate for an enhanced circulation time in the blood.[25] The zeta potential was a slightly negative value (−14.5 mV), and 30% of cholesterol content seems to lower the surface charge of liposomes when considering that the zeta potential of liposomes which are only composed of DPPC is close to neutral (Fig. 3(D)).[26]

Iron-mediated cytotoxicity and involvement of ferroptosis according to iron uptake rate in HK-2 cells

Insufficient studies have been conducted to thoroughly investigate the effects of iron toxicity on kidney cells and the specific mechanisms of cell death that are involved. However, there is a need to determine the mechanisms of iron toxicity on cells to find a proper way to prevent it. So, we tested the toxicity of iron overload on HK-2 cells. FAC is usually used to establish an iron overload model *in vitro*. It is a more stable form of ferric citrate, which is one of the forms of NTBI.[27-29] The cell viability assay results showed that FAC has toxicity in HK-2 cells that is dependent on concentration and time (Fig. 4(A)). And the involvement of ferroptosis in iron overload-induced renal cell death has not been studied. A ferroptosis inhibitor was added before treating with FAC (1 mmol L^{-1}) for 48 h in cells to verify whether ferroptosis is the main cause of FAC-induced cell death. Ferrostatin-1 is known to be a specific ferroptosis inhibitor.[30] The findings

Journal of Chemical Technology and Biotechnology published by John Wiley & Sons Ltd on behalf of Society of Chemical Industry (SCI).

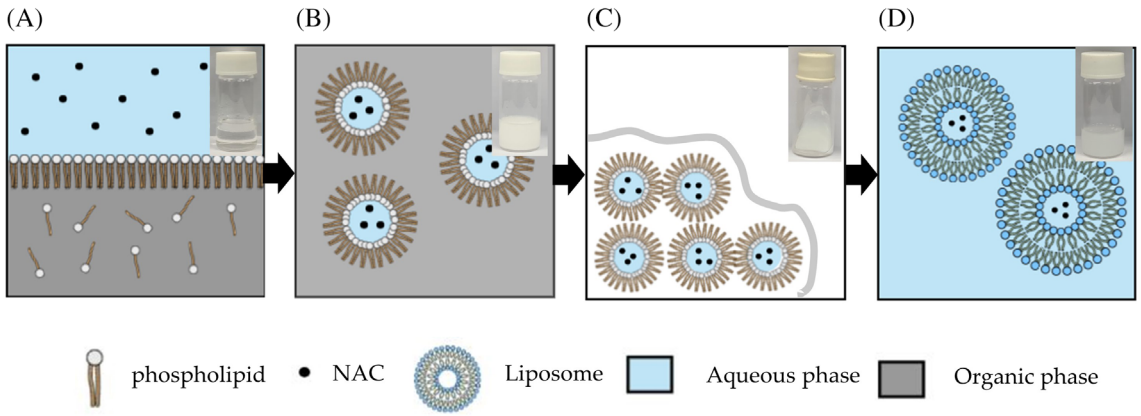

Figure 2. (A) Schematic illustration and images that show the overall REV process. The organic phase (phospholipids and cholesterol) and the aqueous phase (drug) were separated. (B) After sonication, a homogeneous milky solution was seen that shows the W/O emulsion. (C) Organo-gel was formed after evaporation of the organic solvent. (D) Transparent solution of liposomes was seen after serial extrusions.

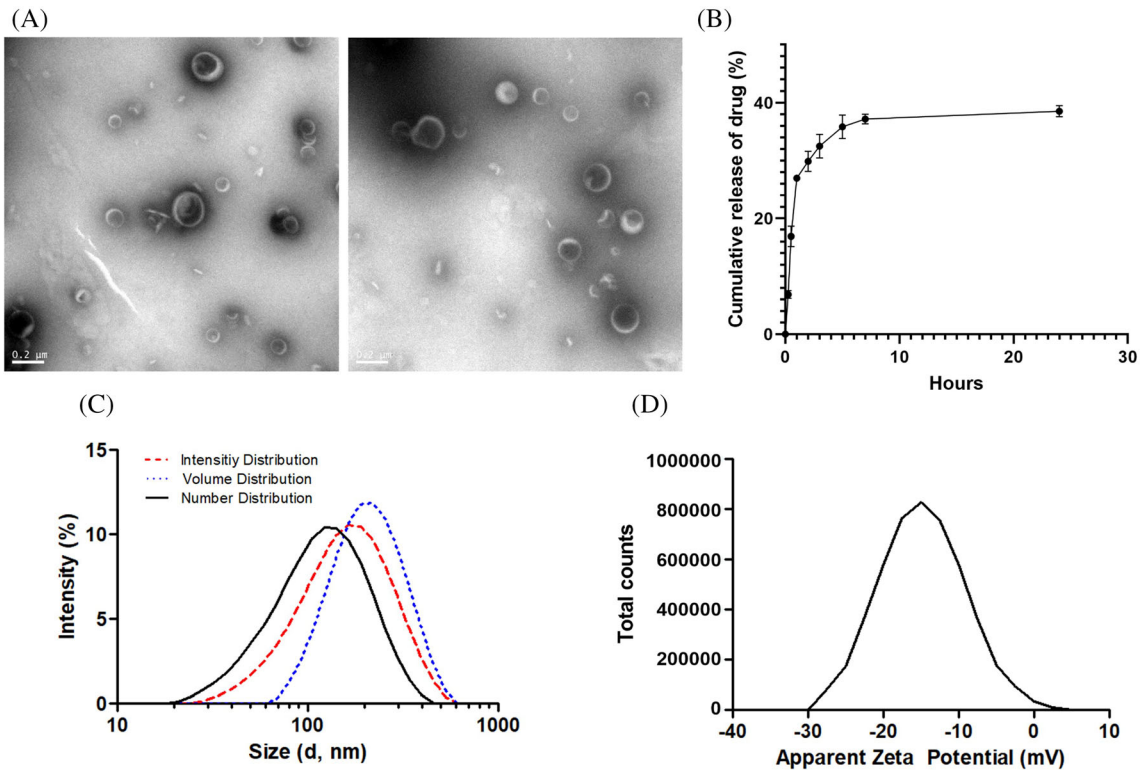

Figure 3. Characterization of liposomal NAC. (A) Morphology of liposomes was confirmed by TEM imaging. (B) Release profile of liposomes in DPBS (pH 7.4) at 37 °C. (C) DLS data showing the size distribution and (D) zeta potential distribution. Data presented show the mean ± SEM ($n = 3$).

demonstrated that the use of ferrostatin-1 effectively inhibited cell death caused by the slow accumulation of iron (supporting information, Fig. S1). However, necrostatin-1 (necrosis inhibitor) and Z-VAD-FMK (apoptosis inhibitor) had little or no protective effect on the iron toxicity (supporting information, Fig. S1). This was a similar result to that of other researches that considered hepatocytes and cancer cells.[4,5] Although some studies indicated that necrosis is also involved in iron overload-induced cell death,[31] these results showed that ferroptosis is the main cause of FAC-induced cell death.

Other researchers designed an iron overload model in T51B rat liver epithelial cells using FAC and 8-Hq to demonstrate the reduction of toxicity caused by iron overload with curcumin. 8-Hq facilitates the cellular uptake of iron when bonding to Fe ions. The rapid uptake of iron, which is shorter than 2 h, can minimize the cellular defense responses to iron overload conditions.[32] Figure 4(B) shows that 8-Hq increased the cytotoxicity of iron within 2 h compared to adding iron alone or 8-Hq alone. Ferrostatin-1 was also treated before adding FAC (50 μmol L^{-1}) and 8-Hq (20 μmol L^{-1}) to confirm the relevance of ferroptosis in this iron overload condition (supporting information, Fig. S1). Interestingly, unlike the results from a significant protective effect of ferrostatin-1 on FAC-induced cell death, ferrostatin-1 did not have a protective effect on cell death induced by FAC and

Journal of Chemical Technology and Biotechnology published by John Wiley & Sons Ltd on behalf of Society of Chemical Industry (SCI).

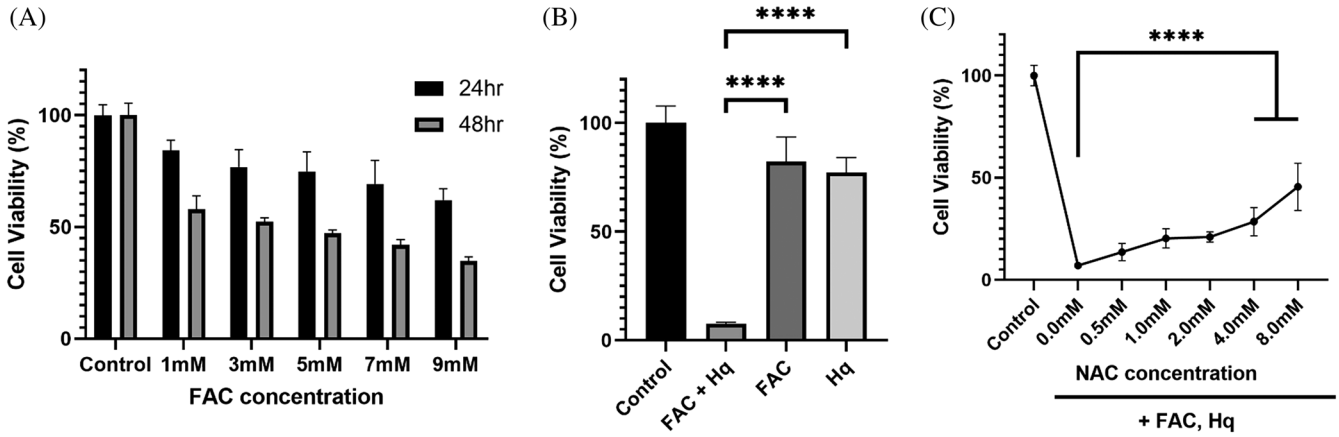

Figure 4. Iron-mediated cytotoxicity in HK-2 cells and NAC having a significant protective effect on cytotoxicity induced by rapid iron uptake. (A) FAC reduced cell viability in a concentration- and time-dependent manner. (B) 8-Hq increased the cytotoxicity of FAC within 2 h. After treatment with 50 μmol L^{-1} FAC and 20 μmol L^{-1} 8-Hq for 2 h, the differences between the two groups were compared. (C) NAC increased cell viability in a concentration-dependent manner. After NAC was added, 50 μmol L^{-1} FAC and 20 μmol L^{-1} 8-Hq were treated for 2 h. Data presented show the mean ± SEM ($n = 5$; ****$P < 0.0001$). Significant statistical differences were verified using a one-way ANOVA test.

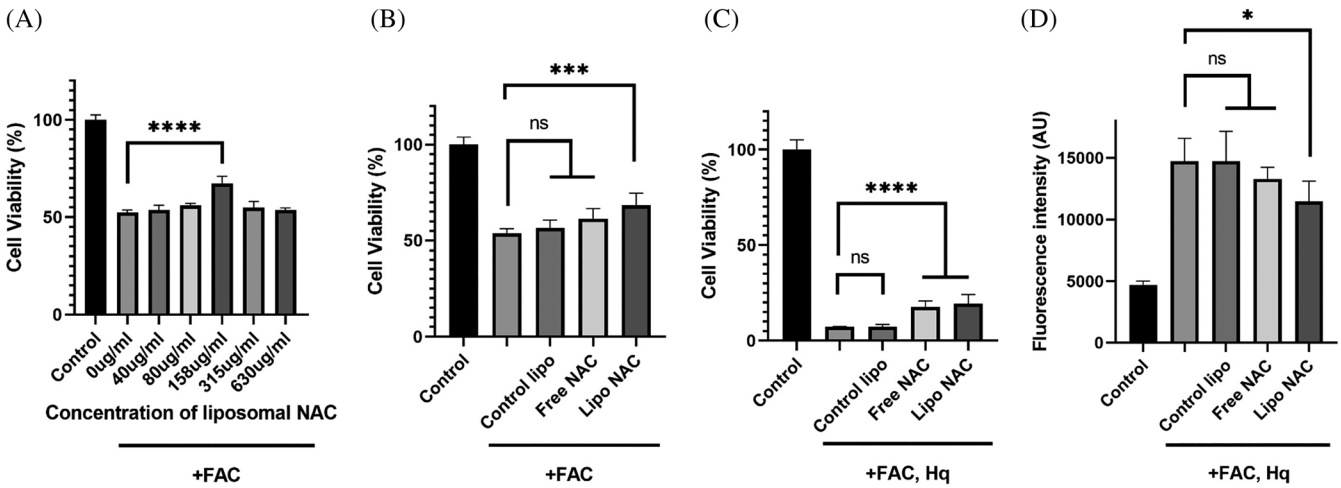

Figure 5. Protective effect of liposomal NAC was shown using cell viability assay and cellular ROS assay in HK-2 cells. (A) Various concentrations of liposomal NAC were added before FAC was treated. (B) Control liposome (157.5 μg mL^{-1}), free NAC (1.5 mmol L^{-1}) and liposomal NAC were added before FAC was treated. FAC (1 mmol L^{-1}) was treated for 48 h. (C) Control liposome, free NAC and liposomal NAC were added before 50 μmol L^{-1} FAC and 20 μmol L^{-1} 8-Hq were treated for 2 h. Cell viability was measured using the CCK-8 assay. (D) Control liposome, free NAC and liposomal NAC were added before 50 μmol L^{-1} FAC and 20 μmol L^{-1} 8-Hq were treated for 30 min. Intracellular ROS was quantified using a DCFDA assay. Data presented show the mean ± SEM ($n = 5$; *$P < 0.05$, ***$P < 0.001$, ****$P < 0.0001$, ns: no significance). Significant statistical differences were verified using a one-way ANOVA test.

8-Hq. This result is similar to previous research that used hepatocytes instead.[5] Necrostatin-1 (necrosis inhibitor) and Z-VAD-FMK (apoptosis inhibitor) also did not recover cell death (supporting information, Fig. S1). However, when NAC was treated overnight, it was found that NAC recovered cell death in a dose-dependent manner (Fig. 4(C)). Considering that NAC is an antioxidant, cell death might be because of a sudden increase of free radicals by rapid cellular uptake of iron ions. However, research will be needed on why a ferroptosis inhibitor, acting by inhibiting lipid peroxidation, cannot recover this cell death.

Protective effect of liposomal NAC on iron-overloaded HK-2 cells

The protective effect of liposomal NAC was confirmed using a cell viability assay and cellular ROS assay. Before treatment with 1 mmol L^{-1} FAC for 48 h on cells to establish the slow iron uptake model, various liposomal NAC concentrations were added overnight. The result showed that 157.5 μg mL^{-1} (about 0.25 mmol L^{-1} lipid concentration) of liposome increased cell viability from 52.3% to 67.38% (Fig. 5(A)). Interestingly, a higher concentration of liposomes did not have a significant protective effect on cells. Therefore, further experiments were done with 157.5 μg mL^{-1} concentration. The liposomal NAC group was compared to the NAC-free control liposome group and a group with an equal amount of free NAC, under the same conditions. Contrary to the control liposomes and free NAC, which did not show a significant protective effect, liposomal NAC recovered the FAC-induced cell death from 53.9% to 68.4% (Fig. 5(B)). For treatment with FAC at 50 μmol L^{-1} and 8-Hq at 20 μmol L^{-1}, liposomal NAC also increased cell viability from 7.2% to 19.4% and had a slightly more improved effect than free NAC (Fig. 5(C)).

Journal of Chemical Technology and Biotechnology published by John Wiley & Sons Ltd on behalf of Society of Chemical Industry (SCI).

And then, the amount of intracellular ROS was quantified using a DCFDA assay kit to verify the anti-oxidative effect of liposomes (Fig. 5(D)). We observed that the Fe–Hq complex induced ROS generation within 30 min, but control liposomes had no significant scavenging effect. Free NAC resulted in only a slight reduction in ROS, suggesting its limited efficacy in scavenging ROS when not encapsulated. Based on these results, liposomal NAC demonstrated a significant reduction in ROS, underscoring its enhanced antioxidative properties when delivered in liposomal form. These results suggest not only that liposomal NAC increases the protective effect of free NAC by facilitating the cellular uptake of hydrophilic drug but also that the released NAC retains significant antioxidant activity that contributes to its overall therapeutic efficacy.[33]

CONCLUSION

We fabricated liposomes that encapsulate antioxidant NAC using a REV method. And an iron overload model was established in HK-2 cells according to the cellular uptake rate of iron. Although ferroptosis is involved in the slow accumulation of intracellular iron, ferroptosis seems to be not involved in the rapid iron uptake condition. However, the liposomal NAC increased the cell viability and decreased ROS generation in both iron overload models. These results imply that liposomal NAC can protect kidney cells from iron overload-induced toxicity, whether or not ferroptosis is involved. Also, the liposomal formulation improved the effect of free NAC by increasing the cellular uptake of hydrophilic drug. This research would help determine the mechanism of cytotoxicity caused by iron overload and how to treat related diseases. However, further research will need to be conducted to determine through which mechanisms NAC acts and whether liposomal NAC has an *in vivo* protective effect.[24]

ACKNOWLEDGEMENTS

This research was supported by a grant of Ministry of Trade, Industry and Energy, Republic of Korea (no. 20018522) and a grant of Korea Health Technology R&D Project through the Korea Health Industry Development Institute (KHIDI), funded by the Ministry of Health & Welfare, Republic of Korea (no. HI22C139400). This work was in part supported by the Research Institute for Convergence Science.

CONFLICT OF INTEREST STATEMENT

The authors declare that they have no known competing financial interests or personal relationships that could have appeared to influence the work reported in this paper.

SUPPORTING INFORMATION

Supporting information may be found in the online version of this article.

REFERENCES

1 Patel M and Ramavataram DV, Non transferrin bound iron: nature, manifestations and analytical approaches for estimation. *Indian J Clin Biochem* **27**:322–332 (2012). https://doi.org/10.1007/s12291-012-0250-7.
2 Brissot P, Ropert M, Le Lan C and Loréal O, Non-transferrin bound iron: a key role in iron overload and iron toxicity. *Biochim Biophys Acta* **1820**:403–410 (2012). https://doi.org/10.1016/j.bbagen.2011.07.014.
3 van Swelm R, Wetzels J and Swinkels DW, The multifaceted role of iron in renal health and disease. *Nat Rev Nephrol* **16**:77–98 (2020). https://doi.org/10.1038/s41581-019-0197-5.
4 Wang H, An P, Xie E, Wu Q, Fang X, Gao H *et al.*, Characterization of ferroptosis in murine models of hemochromatosis. *Hepatology* **66**:449–465 (2017). https://doi.org/10.1002/hep.29117.
5 Fang S, Yu X, Ding H, Han J and Feng J, Effects of intracellular iron overload on cell death and identification of potent cell death inhibitors. *Biochem Biophys Res Commun* **503**:297–303 (2018). https://doi.org/10.1016/j.bbrc.2018.06.019.
6 Xie Y, Hou W, Song X, Yu Y, Huang J, Sun X *et al.*, Ferroptosis: process and function. *Cell Death Differ* **23**:369–379 (2016). https://doi.org/10.1038/cdd.2015.158.
7 Musallam KM and Taher AT, Mechanisms of renal disease in β-thalassemia. *J Am Soc Nephrol* **23**:1299–1302 (2012). https://doi.org/10.1681/ASN.2011111070.
8 Neufeld EJ, Update on iron chelators in thalassemia. *Hematology* **2010**:451–455 (2010). https://doi.org/10.1182/asheducation-2010.1.451.
9 Kose T, Vera-Aviles M, Sharp PA and Latunde-Dada GO, Curcumin and (−)-epigallocatechin-3-gallate protect murine MIN6 pancreatic beta-cells against iron toxicity and erastin-induced ferroptosis. *Pharmaceuticals* **12**:26 (2019). https://doi.org/10.3390/ph12010026.
10 Vera-Aviles M, Vantana E, Kardinasari E, Koh NL and Latunde-Dada GO, Protective role of histidine supplementation against oxidative stress damage in the management of anemia of chronic kidney disease. *Pharmaceuticals* **11**:111 (2018). https://doi.org/10.3390/ph11040111.
11 Tardiolo G, Bramanti P and Mazzon E, Overview on the effects of *N*-acetylcysteine in neurodegenerative diseases. *Molecules* **23**:3305 (2018). https://doi.org/10.3390/molecules23123305.
12 Šalamon Š, Kramar B, Marolt TP, Poljšak B and Milisav I, Medical and dietary uses of *N*-acetylcysteine. *Antioxidants* **8**:111 (2019). https://doi.org/10.3390/antiox8050111.
13 Lu SC, Regulation of glutathione synthesis. *Mol Aspects Med* **30**:42–59 (2009). https://doi.org/10.1016/j.mam.2008.05.005.
14 Wrotek S, Sobocińska J, Kozłowski HM, Pawlikowska M, Jędrzejewski T and Dzialuk A, New insights into the role of glutathione in the mechanism of fever. *Int J Mol Sci* **21**:1393 (2020). https://doi.org/10.3390/ijms21041393.
15 Atkuri KR, Mantovani JJ, Herzenberg LA and Herzenberg LA, *N*-acetylcysteine: a safe antidote for cysteine/glutathione deficiency. *Curr Opin Pharmacol* **7**:355–359 (2007). https://doi.org/10.1016/j.coph.2007.04.005.
16 Santus P, Corsico A, Solidoro P, Braido F, Di Marco F and Scichilone N, Oxidative stress and respiratory system: pharmacological and clinical reappraisal of *N*-acetylcysteine. *COPD* **11**:705–717 (2014). https://doi.org/10.3109/15412555.2014.898040.
17 Olsson B, Johansson M, Gabrielsson J and Bolme P, Pharmacokinetics and bioavailability of reduced and oxidized *N*-acetylcysteine. *Eur J Clin Pharmacol* **34**:77–82 (1988). https://doi.org/10.1007/BF01061422.
18 Alipour M, Buonocore C, Omri A, Szabo M, Pucaj K and Suntres ZE, Therapeutic effect of liposomal-*N*-acetylcysteine against acetaminophen-induced hepatotoxicity. *J Drug Target* **21**:466–473 (2013). https://doi.org/10.3109/1061186X.2013.765443.
19 Mitsopoulos P, Omri A, Alipour M, Vermeulen N, Smith MG and Suntres ZE, Effectiveness of liposomal-*N*-acetylcysteine against LPS-induced lung injuries in rodents. *Int J Pharm* **363**:106–111 (2008). https://doi.org/10.1016/j.ijpharm.2008.07.015.
20 Alipour M, Omri A, Smith MG and Suntres ZE, Prophylactic effect of liposomal *N*-acetylcysteine against LPS-induced liver injuries. *J Endotoxin Res* **13**:297–304 (2007). https://doi.org/10.1177/0968051907085062.
21 Eloy JO, Claro de Souza M, Petrilli R, Barcellos JP, Lee RJ and Marchetti JM, Liposomes as carriers of hydrophilic small molecule drugs: strategies to enhance encapsulation and delivery. *Colloids Surf B* **123**:345–363 (2014). https://doi.org/10.1016/j.colsurfb.2014.09.029.
22 Akbarzadeh A, Rezaei-Sadabady R, Davaran S, Joo SW, Zarghami N, Hanifehpour Y *et al.*, Liposome: classification, preparation, and applications. *Nanoscale Res Lett* **8**:102 (2013). https://doi.org/10.1186/1556-276X-8-102.
23 Yang WS and Stockwell BR, Ferroptosis: death by lipid peroxidation. *Trends Cell Biol* **26**:165–176 (2016). https://doi.org/10.1016/j.tcb.2015.10.014.
24 Szoka F Jr and Papahadjopoulos D, Procedure for preparation of liposomes with large internal aqueous space and high capture by

reverse-phase evaporation. *Proc Natl Acad Sci USA* **75**:4194–4198 (1978). https://doi.org/10.1073/pnas.75.9.4194.
25 Liu D, Mori A and Huang L, Role of liposome size and RES blockade in controlling biodistribution and tumor uptake of GM1-containing liposomes. *Biochim Biophys Acta* **1104**:95–101 (1992). https://doi.org/10.1016/0005-2736(92)90136-a.
26 Magarkar A, Dhawan V, Kallinteri P, Viitala T, Elmowafy M, Róg T *et al.*, Cholesterol level affects surface charge of lipid membranes in saline solution. *Sci Rep* **4**:5005 (2014). https://doi.org/10.1038/srep05005.
27 Messner DJ, Rhieu BH and Kowdley KV, Iron overload causes oxidative stress and impaired insulin signaling in AML-12 hepatocytes. *Dig Dis Sci* **58**:1899–1908 (2013). https://doi.org/10.1007/s10620-013-2648-3.
28 Wheby MS and Umpierre G, Effect of transferrin saturation on iron absorption in man. *N Engl J Med* **271**:1391–1395 (1964). https://doi.org/10.1056/NEJM196412312712704.
29 Grootveld M, Bell JD, Halliwell B, Aruoma OI, Bomford A and Sadler PJ, Non-transferrin-bound iron in plasma or serum from patients with idiopathic hemochromatosis. Characterization by high performance liquid chromatography and nuclear magnetic resonance spectroscopy. *J Biol Chem* **264**:4417–4422 (1989).
30 Skouta R, Dixon SJ, Wang J, Dunn DE, Orman M, Shimada K *et al.*, Ferrostatins inhibit oxidative lipid damage and cell death in diverse disease models. *J Am Chem Soc* **136**:4551–4556 (2014). https://doi.org/10.1021/ja411006a.
31 Yang F, Li Y, Yan G, Liu T, Feng C, Gong R *et al.*, Inhibition of iron overload-induced apoptosis and necrosis of bone marrow mesenchymal stem cells by melatonin. *Oncotarget* **8**:31626–31637 (2017). https://doi.org/10.18632/oncotarget.16382.
32 Messner DJ, Sivam G and Kowdley KV, Curcumin reduces the toxic effects of iron loading in rat liver epithelial cells. *Liver Int* **29**:63–72 (2009). https://doi.org/10.1111/j.1478-3231.2008.01793.x.
33 Hoesel LM, Flierl MA, Niederbichler AD, Rittirsch D, McClintock SD, Reuben JS *et al.*, Ability of antioxidant liposomes to prevent acute and progressive pulmonary injury. *Antioxid Redox Signal* **10**:973–981 (2008). https://doi.org/10.1089/ars.2007.1878.